

## Wannier excitons in the ferromagnetic semiconductors EuO and EuS

Tadaoki Mitani and Takao Koda

*Department of Applied Physics, Faculty of Engineering, University of Tokyo, Hongo, Bunkyo-ku, Tokyo, 113 Japan*

(Received 12 August 1974)

Fine structures in the thermorefectance (TR) spectra of EuO and EuS in the ultraviolet region are ascribed for the first time to Wannier excitons in magnetic semiconductors. The characteristic temperature-induced splittings of the spectra of EuO and EuS at the ferromagnetic spin-ordering temperatures are successfully analyzed in terms of the exciton and the spin-polarization effect of the relevant one-electron bands, an *s*-like conduction and *p*-like valence bands, at the  $\Gamma$  point. The magnetic-spin-exchange energies,  $J_c$  and  $J_v$ , between the localized Eu-4*f* electrons and the band electrons, the spin-orbit interaction energy  $\lambda$  for the valence band, and the electron-hole spin-exchange energy  $\Delta$  for the exciton are estimated. It is demonstrated that the TR measurements open a new aspect of the optical study of magnetic-semiconductor excitons which become an ideal probe for directly detecting the interaction between the localized-magnetic-spin system and the nonlocalized-Bloch-electron system in the magnetic semiconductors.

### I. INTRODUCTION

The effects of magnetic-spin ordering on the nonlocalized Bloch electrons are a central subject in the study of magnetic semiconductors. A number of investigations have already been undertaken with regard to this subject in the Eu chalcogenides.<sup>1</sup> However, the quantitative details of the one-electron bands and the effect of the magnetic-spin ordering on the Bloch electrons have not yet been studied extensively with all the methods of semiconductor spectroscopy.

It was with the hope of obtaining more direct information on their band structure that we initiated thermorefectance (TR) measurements on the Eu chalcogenides. When applied to the optical spectra of these magnetic semiconductors near the magnetic-phase-transition temperature, the TR technique proved to be particularly powerful in its ability to reveal fine structures of the spectra which were previously not resolved in the ordinary reflection measurements.<sup>2</sup> The most noticeable result of the TR measurement was the doublet structure found in the uv region for all Eu chalcogenides in the paramagnetic phase. From the characteristic temperature dependence of the signals at the ferro- and antiferromagnetic-phase transitions, we have speculated that the doublet is ascribable to the Wannier-type excitons associated with the  $\Gamma_{15v} - \Gamma_{1c}$  band edge of these semiconductors.<sup>3</sup>

The purpose of this paper is to present a theoretical analysis of the above doublet in ferromagnetic EuO and EuS, based upon the recent advances in exciton studies.<sup>4</sup> The substantial changes of the doublet at the ferromagnetic-spin-ordering temperature are successfully accounted for in terms of a Wannier exciton and the spin polarization of the relevant one-electron bands. It is dem-

onstrated that in a magnetic semiconductor the Wannier exciton is quite useful as a microscopic probe to detect the exchange interaction between the localized magnetic spin and nonlocalized Bloch electrons.

### II. EXPERIMENTAL RESULTS

A small platelet sample of Eu chalcogenide single crystal (about  $2 \times 2 \times 0.1$  mm<sup>3</sup> in size) was glued on a thin stainless steel sheet (about 1.5  $\mu$ m thick). The stainless steel sheet was used as a heater by passing a pulsed current of up to about 0.8 A. The duty cycle of the pulse was 0.09 sec, and the pulse width was 0.3 msec. Because of the small heat capacity of the sample and the heater, about 1 mW was sufficient to produce a temperature modulation  $\Delta T \approx 0.1$  °C, without appreciably raising the average temperature of the sample. The TR spectra  $\Delta R/R$  were measured by a Spex 1704 monochromator combined with a Xe discharge lamp, an EMI 6256S photomultiplier, and a lock-in amplifier.

The sample was mounted within a variable-temperature optical cryostat. The sample temperature was determined from the thermal shift of the unmodulated reflectivity in the spectral region where the reflectivity is strongly temperature dependent. By calibrating the shift of the spectra at several fixed temperatures, the temperature change of the sample could be determined with an accuracy of about 0.05 °C at the spot on the sample surface where the TR measurements were being made. The accuracy of the absolute temperature was about 0.1 °C.

The TR signals in the uv region (referred to as the *C* signals in Refs. 2 and 3) are shown in Fig. 1(a) for EuO and in Fig. 2 for EuS, respectively. The TR signals  $\Delta R/R$  are denoted as being positive when *R* increases with temperature.

## III. DISCUSSIONS

## A. General consideration

As shown in Fig. 1(a) and Fig. 2, the TR spectra in the paramagnetic region of both compounds ( $T > 69.4$  K for EuO and  $T > 16.5$  K for EuS) are composed of well-separated doublet peaks at about 4.76 and 5.17 eV in EuO and at about 4.15 and 4.32 eV in EuS, respectively.

The most noticeable feature of the doublet is the drastic change it undergoes at the ferromagnetic-spin-ordering temperature. For example, as the temperature is lowered from about 100 K, the intensity of the doublet in EuO increases. At the same time, the peaks shift slightly to lower energy without changing the doublet separation. When the temperature reaches the ferromagnetic-spin-ordering temperature  $T_c = 69.4$  K, the spectrum changes abruptly and the doublet splits into a multiple component structure. A similar change with temperature of the doublet is also observed in EuS, as shown in Fig. 2. In order to illustrate the characteristic temperature dependence of the TR

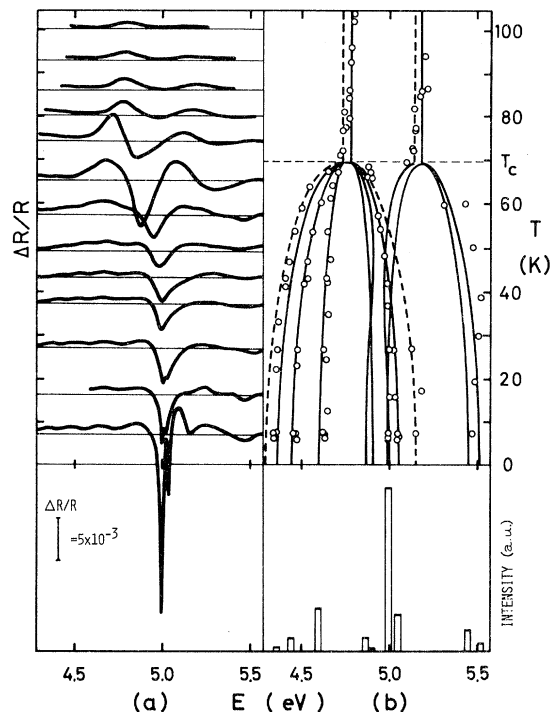


FIG. 1. (a) Ultraviolet thermorefectance spectra of EuO. Respective temperatures are indicated by the vertical positions of curves along the ordinate. Scale for the TR signals is indicated by a vertical bar corresponding to  $\Delta R/R = 5 \times 10^{-3}$ . (b) Upper: Experimental points (open circles) and calculated exciton levels (solid and broken lines for the dipole-allowed and -forbidden excitons, respectively). Lower: Calculated relative intensities of excitons at  $T = 0$ .

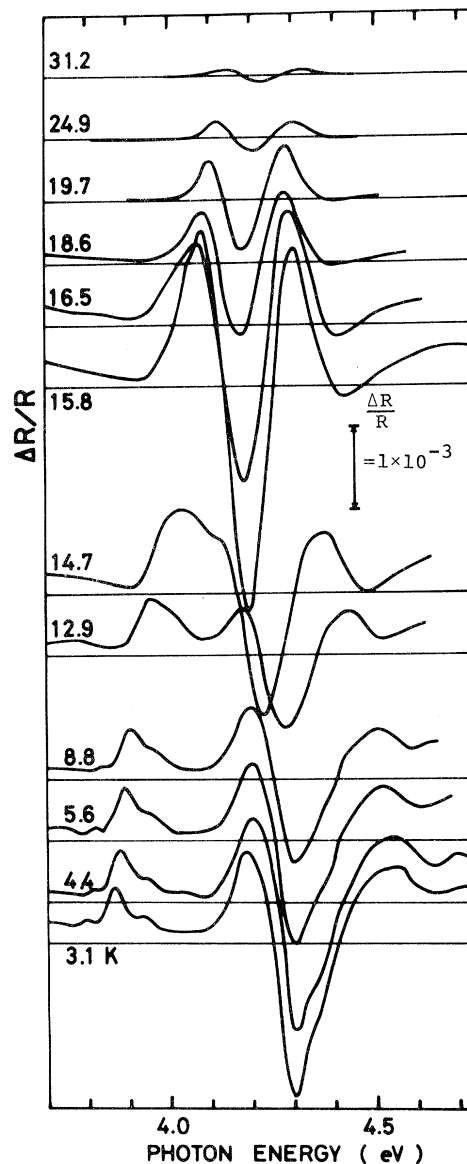


FIG. 2. Ultraviolet thermorefectance spectra of EuS. Scale for the TR signals is indicated by a vertical bar corresponding to  $\Delta R/R = 10^{-3}$ .

signals more clearly, we have plotted the specific energies of the TR signals at various temperatures across  $T_c$  in Fig. 1(b) and Fig. 3. These experimental points (the open circles) were taken at the maximum points for the structures showing red shift and at the minimum points for the structures exhibiting blue shift with decreasing temperature. Looking at the plots, we immediately notice that the doublet components in the paramagnetic region split into multiple lines exactly at  $T_c$  in both EuO and EuS.

For the sake of convenience, we briefly summarize here the features of the corresponding TR

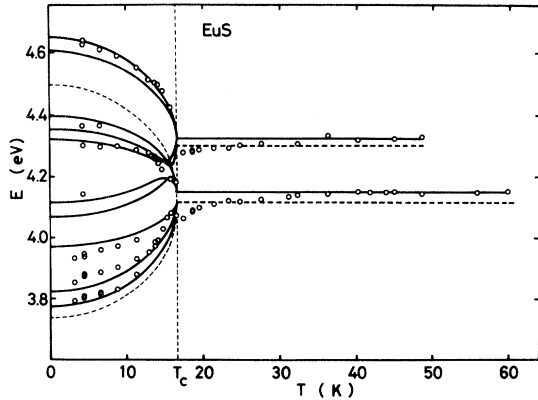


FIG. 3. Experimental points (open circles) and calculated exciton levels (solid and broken lines for the dipole-allowed and -forbidden excitons, respectively) for EuS.

signals in EuSe and EuTe. Doublet structures were observed at 3.90 and 4.23 eV in EuSe and at about 3.48 and 3.90 eV in EuTe.<sup>3</sup> The intensities of the doublet components change rather abruptly at around  $T_N$  (4.6 K for EuSe and 9.6 K for EuTe), but no overall splitting was observed at  $T_N$ , in marked contrast with the remarkable doublet splitting in EuO and EuS at  $T_c$ . Quantitative discussions of these doublets in antiferromagnetic EuSe and EuTe will be given in a separate paper, along with the results of magneto-modulation measurements presently under way.

Among the several possibilities for the origin of the doublet, the most natural one will be an interpretation in which the doublet is related to the spin-orbit partners of direct exciton associated with an  $s$ -like conduction and  $p$ -like valence bands. It is noted that the separations of the exciton doublet in Ba chalcogenides, having the same valence-electron configuration as the Eu chalcogenides, are of the right order of magnitude and show a similar chalcogen dependence to the TR doublet separations in the Eu chalcogenides and therefore support this interpretation. They are reported to be about 0.28 eV for BaO, 0.15 eV for BaS, 0.35 eV for BaSe, and 0.55 eV for BaTe.<sup>5</sup> The corresponding spacings of the TR doublet are 0.41 eV for EuO, 0.17 eV for EuS, 0.33 eV for EuSe, and 0.42 eV for EuTe. (The appreciable deviation of the value for BaO from a regular chalcogen-dependent sequence has been ascribed by Krumhansl to be the contribution of the cation orbitals in the valence band.<sup>6</sup> Presumably, a similar mechanism might explain the large doublet separation in EuO.)

Furthermore, it was found that the observed shapes of the TR doublet could be accounted for by the Lorentz oscillator model.<sup>3</sup> This model has been successfully applied by Matatagui *et al.*<sup>7</sup> for

a line-shape analysis of the TR spectra due to the parabolic excitons in compound semiconductors. Thus all of the data strongly suggest that it is appropriate to adopt the Wannier exciton model for describing the observed TR doublets in the Eu chalcogenides. This is quite natural, since the exciton effect is known to play an essential role in the band-edge spectra of compound semiconductors because of the strong Coulomb interaction between the photoexcited Bloch electron and hole. In Sec. III B, we develop a theoretical consideration to show that the exciton theory is not only sufficient but is necessary to analyze the observed splitting of the doublet at  $T_c$  of EuO and EuS, as shown in Figs. 1(b) and 3.

### B. Theoretical analysis of the results

As the first step in our discussion of the exciton model, we consider a one-electron band structure consisting of a  $p$ -like valence band and an  $s$ -like conduction band, both having the extrema at  $k=0$ . In the paramagnetic phase, the conduction band ( $\Gamma_{6+}$ ) is doubly degenerate because of the spin, while the valence band is split into fourfold degenerate  $\Gamma_{8-}$  ( $j=\frac{3}{2}$ ) and twofold degenerate  $\Gamma_{6-}$  ( $j=\frac{1}{2}$ ) bands by the spin-orbit interaction. When a ferromagnetic-spin ordering takes place, the conduction band splits into up and down spin-polarized bands, and the valence bands split into six nondegenerate bands under the combined effect of the spin-orbit interaction and the magnetic exchange interaction with the localized Eu-4*f* electrons. The energy-level scheme of the spin-polarized bands is treated by a theoretical framework, as described in the Appendix and is schematically illustrated in Fig. 4 as a function of temperature across  $T_c$ . For an antiferromagnetic spin ordering, there should be no band splitting.

We proceed then by making a working hypothesis that the observed TR signals are ascribable to the

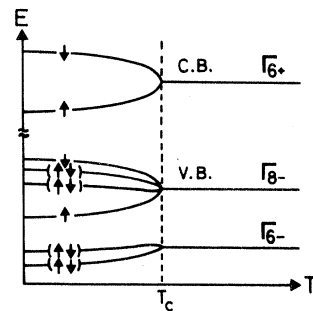


FIG. 4. Schematic energy levels of the spin-polarized  $s$ -like conduction and  $p$ -like valence bands in a ferromagnetic semiconductor. Single (double) arrows indicate pure (mixed)-spin magnetic subbands.

Wannier excitons associated with these valence and conduction bands. This model is compatible with the aforementioned facts, i. e., a similarity of the TR doublets to the exciton doublets in the Ba chalcogenides and the applicability of the Lorentz oscillator model, which is known to be adequate for a phenomenological description of the Wannier exciton in ionic crystals.<sup>7,8</sup>

Theoretical procedures needed to calculate the exciton states associated with the  $p$ -like valence and  $s$ -like conduction bands at  $k=0$  have been developed by Onodera and Toyozawa for alkali halides.<sup>9</sup> The possible exciton energies in the Eu chalcogenides in the paramagnetic phase are likewise obtained by taking account of the spin-orbit interaction of the valence band and the electron-hole spin-exchange interaction. Out of the twelve possible electron-hole pairs involving the  $\Gamma_{6+}$  conduction and the  $\Gamma_{8-}$ ,  $\Gamma_{6-}$  valence bands, we obtain two optically active excitons, each of which has a three-fold degeneracy. The remained six pairs belong to the dipole-forbidden spin-triplet excitons. We assume that the TR doublet observed in the paramagnetic phase of the Eu chalcogenides is due to the two dipole-allowed exciton transitions.

The effect of a ferromagnetic-spin ordering on the exciton states can be formally treated in the same framework as applied to the paramagnetic phase by introducing the spin- and temperature-dependent magnetic exchange energies in the conduction and valence bands (see Appendix). In the present analysis, we assume that the magnetic exchange energies are proportional to the bulk magnetization curve,  $\langle S_z \rangle (T/T_c)/S$ , as calculated by Callen and Callen,<sup>10</sup> where  $S = \frac{7}{2}$  for  $\text{Eu}^{2+}$ , and  $\langle S_z \rangle$  is the thermal average of the  $z$  component of the Eu-4f spin. The proportional constants  $J_c$  for the conduction band and  $J_v$  for the valence band, are to be determined experimentally. We neglect the effect of the short-range spin correlation and the possible difference in the exciton binding energies associated with different bands. Under these simplified conditions, the exciton eigenstates in both para- and ferro-magnetic phases are derived by diagonalizing the  $12 \times 12$  exciton matrix (Appendix, A13), which is formed on the bases of twelve electron-hole (or missing electron) pairs between the two conduction and six valence-band magnetic sublevels.

In the present formalism, the energies and the relative intensities of the excitons are determined in terms of the four adjustable parameters; the valence-band spin-orbit interaction energy  $\lambda$ , the conduction electron-valence-hole spin-exchange energy  $\Delta$ , the aforementioned magnetic exchange constants  $J_c$  and  $J_v$  between the localized Eu-4f spin and the band electrons. The procedure used to determine these parameters was as follows:

TABLE I. Experimental values for the magnetic exchange energies  $J_c$  and  $J_v$  for the conduction and valence bands, respectively; the spin-orbit interaction energy  $\lambda$  for the valence band; and the electron-hole spin-exchange energy  $\Delta$  for the exciton.

	$T_c$ (K)	$J_c$ (eV)	$J_v$ (eV)	$\lambda$ (eV)	$\Delta$ (eV)
EuO	69.4	$0.17 \pm 0.01$	$0.08 \pm 0.01$	$\sim 0.42$	$\sim 0.09$
EuS	16.5	$0.16 \pm 0.01$	$0.06 \pm 0.01$	$\sim 0.19$	$\sim 0.06$

In the paramagnetic region, where  $\langle S_z \rangle (T/T_c) = 0$ , the exciton energies are simply dependent on the two parameters  $\lambda$  and  $\Delta$ . These parameters are determined from the observed separation and the relative intensities of the doublet signals in a manner similar to that used by Onodera and Toyozawa for the halogen-doublet excitons in alkali halides.<sup>9</sup> As discussed by these authors, the doublet separation is mainly governed by the spin-orbit interaction energy  $\lambda$ , while the relative intensities of the doublet components are sensitive to the electron-hole exchange interaction energy  $\Delta$ . By virtue of the modulation technique, it is possible to determine the doublet separation with considerable precision. Estimates for the relative intensity ratio of the doublet components are not so accurate. The experimental values of  $\lambda$  and  $\Delta$  derived in this way are listed in Table I for EuO and EuS. With use of these results, the remaining two parameters  $J_c$  and  $J_v$  are determined in the following way: When temperature is lowered below  $T_c$ , the exciton levels, which are degenerate in the paramagnetic region, are subjected to splitting into twelve nondegenerate exciton levels, as mentioned before. By adjusting the values for  $J_c$  and  $J_v$ , the calculated curves were best fitted to the experimental points below  $T_c$ . This procedure allowed us to make an almost unique determination of the values for  $J_c$  and  $J_v$ . The results are given in Table I. The calculated exciton energies are shown in Fig. 1(b) and Fig. 3 by solid and broken lines for the optically allowed and forbidden exciton levels, respectively. The agreements are quite satisfactory for both EuO and EuS.

As a further confirmation of the present model, we also calculated the relative intensities of the split components at  $T=0$ . Whereas the overall splitting pattern of the doublet is predominantly determined by  $J_c$  and  $J_v$ , the relative intensities of the components are sensitively affected by  $\lambda$  and  $\Delta$ . For example, if  $\lambda$  and  $\Delta$  were zero, only six out of the twelve exciton levels would be dipole allowed, the remaining six being optically inactive pure spin-triplet excitons. Actually, in the presence of the spin-orbit and exchange interactions, these exciton states are mixed to form ten optically active [solid lines in Fig. 1(b) and Fig. 3] and two

dipole-forbidden (broken lines) excitons. The latter two excitons correspond to the pure spin-triplet excitons associated with the two valence-band sublevels with pure spin (the first and the fourth from the top, see Fig. 4). As a result of the mixing, the relative intensities are quite sensitive to the values adopted for  $\lambda$  and  $\Delta$ , providing a suitable way of crosschecking the results derived in the paramagnetic region. The calculated intensities are indicated in the lower part of Fig. 1(b). Note that the largest intensity is predicted for a nearly degenerate exciton level at 5.00 eV. Experimentally, a very strong negative TR signal is observed at the same energy at low temperatures [see Fig. 1(a)], in good agreement with the above prediction. The spectacular changes in the TR spectra of EuO at low temperatures can be explained by the temperature-dependent oscillator strengths of the exciton levels due to the mixing of spin-singlet and triplet components. Since the electron-hole exchange energy  $\Delta$  plays a predominant role in this mixing effect, the semiquantitative agreement of the calculated intensities with the experimental results is regarded as a confirmation of the correctness of the  $\Delta$  value presently adopted. [In Fig. 1(b), some experimental points appear to fall on a broken line corresponding to a forbidden exciton. At the present stage, however, we have no definite explanation for the possibility that the pure spin-triplet exciton becomes optically active.] A similar calculation is also found valid for EuS.

As for the quantitative results assembled in Table I, the value of  $J_c = 0.17$  eV for EuO is reasonable, compared with a theoretical estimation,  $J_c(k=0) = 0.188$  eV, by Rys *et al.*<sup>11</sup> We find that  $J_c$  is nearly independent of chalcogen, as is expected since the  $s$ - $f$  exchange takes place between the Eu- $4f$  electrons and the conduction band dominantly composed of Eu- $6s$  orbital. The smaller value of  $J_v$  and its chalcogen dependence are understandable too, as the  $p$ - $f$  exchange between the Eu- $4f$  electrons and the anion  $p$ -like valence band is responsible for  $J_v$ . The spin-orbit interaction energy  $\lambda$  and the electron-hole exchange energy  $\Delta$  are of reasonable magnitude in comparison with the corresponding quantities in the nonmagnetic halides and chalcogenides.<sup>9,12</sup>

Finally, we would like to make the following two remarks: First, we have entirely ignored the effect of a short-range spin correlation in the present analysis. However, this effect is by no means negligible near  $T_c$  and gives rise to the energy shift of the band extrema, as discussed by several authors.<sup>11,13</sup> In fact, the experimental points in the paramagnetic region deviate appreciably towards lower energy from the calculated lines near  $T_c$  [see Fig. 1(b) and Fig. 3]. This deviation is considered to be due to the effect of the short-range spin correla-

tion on the Bloch electrons; the rate of the observed temperature shift of the doublet slightly above  $T_c$  is about 4 meV/K for EuO and about 5 meV/K for EuS, which are in a reasonable agreement with the energy gain of the conduction-band minimum by the short-range-spin correlation effect calculated by Rys *et al.*<sup>11</sup> for EuO. Second, it should be mentioned here that there exists a considerable background in the unmodulated uv reflection (and absorption) spectra in the energy region where the exciton structures were observed.<sup>14,15</sup> In contrast to the well-developed exciton spectra at the absorption edge of the Ba chalcogenides,<sup>5,12</sup> the whole uv reflection band of the Eu chalcogenides is composed of a strong background and a relatively weak exciton fine structures superposed on it. The origin of this background is considered most likely to be due to the transitions involving the localized Eu- $4f$  electrons—either  $4f^7 \rightarrow 4f^6 5d(e_g)$  transitions as discussed by Scouler *et al.*<sup>15</sup> or else the magnetic excitons similar to that proposed for the band in the visible region.<sup>16</sup> The existence of the overlapping transitions will result in an appreciable lifetime broadening of the exciton spectra, which might explain the difficulty to observe the exciton structure directly in the unmodulated reflection spectra of the Eu chalcogenides. However, by differentiating the whole spectra with respect to temperature, we are able to pick up the exciton-related fine structures almost exclusively out of the background, because the exciton structures are much more sensitive to temperature than the background spectra. In this sense, the TR measurements are especially effective for a selective detection of the Wannier excitons in a magnetic semiconductor, owing to the fact that the spectral shapes and energies of the excitons become strongly temperature sensitive near the magnetic-phase-transition temperature. The critical fluctuation of the localized magnetic spins appears to play an important role in the thermal modulation mechanism.

#### IV. SUMMARY

The TR signals in EuO and EuS are ascribed for the first time to Wannier excitons in magnetic semiconductors. We have found a number of experimental facts, both quantitative and qualitative, which are successfully accounted for by the exciton model. These results altogether lead us to the almost unique conclusion that the exciton theory as presented here is the necessary one to describe the observed TR spectra of EuO and EuS in the uv region. Other interpretations, such as the transitions at a one-electron-band singularity without the exciton effect or those involving the localized Eu- $4f$  electrons, are entirely inapplicable to explain the observed temperature changes of the TR

spectra. As demonstrated in the present study on EuO and EuS, these exciton spectra can be utilized as a microscopic probe to detect the interaction between the localized magnetic spin system and the nonlocalized one-electron band. The TR measurements opened new possibilities for the optical study of the magnetic semiconductor excitons. Through a theoretical analysis of the critical change of the spectra near  $T_c$ , we could obtain quantitative informations on  $J_c$ ,  $J_{\nu}$ , and  $\lambda$ ,  $\Delta$ , which have been inaccessible in previous studies.

#### ACKNOWLEDGMENTS

We are grateful to Dr. T. B. Reed, Lincoln Laboratories, MIT (for EuO and EuS) and to Dr. T. Nakayama, Broadcasting Science Research Laboratories, NHK (for EuS) for kindly supplying us with single-crystal samples. We are also indebted to Professor Y. Onodera, Tokyo Metropolitan University and to Dr. H. Fujita, RCA Research Laboratory, Tokyo, for a critical reading of the manuscript.

#### APPENDIX

Here we formulate a theoretical framework for the Wannier excitons in a ferromagnetic semiconductor. As described in the text, the excitons are postulated to be associated with the one-electron band edge consisting of the  $p$ -like valence ( $\mu$ ) and  $s$ -like conduction ( $\nu$ ) bands, both having the extrema at  $k=0$ .

For the one-electron band states, the bases of the valence band are represented by the following six Bloch functions including the spin function, which is written as  $\uparrow$  for the up-spin and as  $\downarrow$  for the down-spin state:

$$\{b_{\mu}\} = \{p_1 \uparrow, p_1 \downarrow, p_0 \uparrow, p_0 \downarrow, p_{-1} \uparrow, p_{-1} \downarrow\}. \quad (\text{A1})$$

The suffix  $\pm 1$  or 0 for  $p$  indicates the  $z$  component of the orbital angular momentum of the  $p$ -like Bloch bases. The energies of the valence bands are given, in matrix form, by

$$H_{\mu\mu}^{\nu} = \{H^{\nu}(\vec{k})\}_{\mu\mu} \delta_{\mu\mu} + \{H_{\text{so}}^{\nu}\}_{\mu\mu} + \{H_I^{\nu}\}_{\mu\mu}. \quad (\text{A2})$$

The first term corresponds to the kinetic energy of a valence electron, the second term,  $H_{\text{so}}^{\nu} = \frac{2}{3} \lambda \vec{L} \cdot \vec{S}$ , is the spin-orbit interaction,  $\lambda$  being the spin-orbit splitting of the valence bands. The last term,  $H_I^{\nu} = -(V/N) \sum_j J^{\nu}(\vec{r} - \vec{R}_j) \vec{s} \cdot \vec{S}_j$ , is the magnetic exchange interaction between a valence-electron spin  $\vec{s}$  at  $\vec{r}$  and a localized Eu-4 $f$  spin  $\vec{S}_j$  ( $|\vec{S}_j| = \frac{7}{2}$ ) at  $\vec{R}_j$ ,  $J^{\nu}(\vec{r} - \vec{R}_j)$  being the  $p$ - $f$  exchange coupling constant. Retaining only the first-order change in the exchange energy due to the long-range magnetic spin ordering, the last term can be written

$$\{H_I^{\nu}\}_{\mu\mu} = -(1/N) J_{k=0}^{\nu} \sum_j \langle \sigma | \vec{s} \cdot \vec{S}_j | \sigma' \rangle \delta_{\mu\mu}$$

$$= -\frac{1}{2} \sigma J_{k=0}^{\nu} \langle S_z \rangle \delta_{\mu\mu}. \quad (\text{A3})$$

Here,  $J_k^{\nu}$  is the Fourier transform of  $J^{\nu}(\vec{r} - \vec{R}_j)$  and is given by

$$J_k^{\nu} = \int d\vec{r} J^{\nu}(\vec{r} - \vec{R}_j) \exp[-i\vec{k} \cdot (\vec{r} - \vec{R}_j)]. \quad (\text{A4})$$

$\{H_I^{\nu}\}_{\mu\mu}$  is responsible for the spin polarization of the valence bands and is a function of  $T/T_c$  through the temperature-dependent bulk magnetization  $\langle S_z \rangle (T/T_c)$ .

Likewise, on the bases of the  $s$ -like Bloch functions,

$$\{b_{\nu}\} = \{s \uparrow, s \downarrow\}, \quad (\text{A5})$$

the energies of the conduction band are given by

$$H_{\nu\nu}^c = \{H^c(\vec{k})\}_{\nu\nu} \delta_{\nu\nu} + \{H_I^c\}_{\nu\nu}. \quad (\text{A6})$$

Here, the second term represents the spin polarization of the conduction band and is given by

$$H_I^c(T/T_c) = -\frac{1}{2} \sigma J_{k=0}^c \langle S_z \rangle (T/T_c), \quad (\text{A7})$$

$J_k^c$  being the  $s$ - $f$  exchange coupling constant.

The eigenstates of the Wannier excitons that are associated with these valence and conduction bands are expressed as linear combinations of the valence-hole [ $b_{\mu}^*(\vec{r}_h)$ ]-conduction-electron [ $b_{\nu}(\vec{r}_e)$ ] pairs. According to the theoretical formalism for the  $\Gamma$ -excitons associated with the degenerate bands,<sup>9</sup> the wave function of the exciton with the total wave vector  $\vec{K}$  and the internal quantum number  $n$  is given by

$$\psi_{n\vec{K}}(\vec{r}_e - \vec{r}_h) = \sum_{\mu\nu} \exp[\frac{1}{2} i\vec{K} \cdot (\vec{r}_e + \vec{r}_h)] \times F_{\mu\nu}^{n\vec{K}}(\vec{r}_e - \vec{r}_h) b_{\mu}^*(\vec{r}_h) b_{\nu}(\vec{r}_e). \quad (\text{A8})$$

The envelope function  $F_{\mu\nu}^{n\vec{K}}(\vec{r})$  satisfies the following effective-mass equation:

$$\sum_{\mu'\nu'} H_{\mu\nu;\mu'\nu'} F_{\mu'\nu'}^{n\vec{K}}(\vec{r}) = E_n(\vec{K}) F_{\mu\nu}^{n\vec{K}}(\vec{r}), \quad (\text{A9})$$

where

$$H_{\mu\nu;\mu'\nu'} = \delta_{\mu\mu'} H_{\nu\nu}^c + (\frac{1}{2} \vec{K} - i\vec{\nabla}) - H_{\mu\mu}^{\nu} (-\frac{1}{2} \vec{K} - i\vec{\nabla}) \delta_{\nu\nu'} + \delta_{\mu\mu'} \delta_{\nu\nu'} V(\vec{r}) + \Omega \delta(\vec{r}) J_{\mu\nu;\mu'\nu'}(\vec{K}). \quad (\text{A10})$$

$V(\vec{r})$  is the attractive Coulomb interaction and the last term is the spin-exchange interaction between the electron and hole,  $\Omega$  being the unit-cell volume. Hereafter, we consider only the ground-state exciton  $n=1S$ .

As the bases of the exciton matrix, we take the form of  $\{p_m s \chi_S\}$ . Here  $p_m$  and  $s$  are the orbital parts of the Bloch functions representing a missing valence electron and a conduction electron, respectively. The spin part  $\chi_S$  is written, for the

spin-singlet ( $S=0$ ) and spin-triplet ( $S=1$ ) state, as

$$\chi_{S=0, S_z=0} = (1/\sqrt{2})(|\uparrow\uparrow\rangle + |\downarrow\downarrow\rangle)$$

for the spin-singlet, and

$$\begin{aligned} \chi_{S=1, S_z=+1} &= |\uparrow\uparrow\rangle, \\ \chi_{S=1, S_z=0} &= (1/\sqrt{2})(|\uparrow\downarrow\rangle - |\downarrow\uparrow\rangle), \\ \chi_{S=1, S_z=-1} &= |\downarrow\downarrow\rangle, \end{aligned} \quad (\text{A11})$$

for the spin-triplet exciton. By use of these bases, the electron-hole exchange energy is approxi-

mately given by

$$\Delta = \begin{cases} \delta_{\mu\mu'}\delta_{\nu\nu'}2J|F(0)|^2\Omega, & \text{for } S=0 \\ 0, & \text{for } S=1. \end{cases} \quad (\text{A12})$$

$J$  is the exchange integral for the transverse exciton state.<sup>9</sup>

The eigenstates of the excitons are derived from the effective-mass equation [(A9), (A10)]. In particular, the energy spectrum of the excitons is obtained by diagonalizing the  $12 \times 12$  exciton matrix formed on the bases of  $\{p_m^S \chi_{S_z}\}$ , which is written as

$$H_{\mu\nu\mu'\nu'} = \begin{array}{cccc|cccc|cccc} \Delta & -\Lambda + \Sigma' & -\Lambda & & & & & & & & & & & & & & & (p_{1^S} \chi_{0,0}) \\ -\Lambda + \Sigma' & 0 & \Lambda & & & & & & & & & & & & & & & & (p_{1^S} \chi_{1,0}) \\ -\Lambda & \Lambda & \Sigma & & & & & & & & & & & & & & & & (p_{0^S} \chi_{1,1}) \\ & & & \Delta & \Sigma' & -\Lambda & -\Lambda & & & & & & & & & & & & (p_{0^S} \chi_{0,0}) \\ & & & \Sigma' & 0 & -\Lambda & \Lambda & & & & & & & & & & & & (p_{0^S} \chi_{1,0}) \\ & & & -\Lambda & -\Lambda & \Lambda - \Sigma & 0 & & & & & & & & & & & & (p_{1^S} \chi_{1,-1}) \\ & & & -\Lambda & \Lambda & 0 & \Lambda + \Sigma & & & & & & & & & & & & (p_{-1^S} \chi_{1,1}) \\ & & & & & & & \Delta & \Lambda + \Sigma' & -\Lambda & & & & & & & & & (p_{-1^S} \chi_{0,0}) \\ \Lambda + \Sigma' & 0 & -\Lambda & & & & & \Lambda + \Sigma' & 0 & -\Lambda & & & & & & & & & (p_{-1^S} \chi_{1,0}) \\ -\Lambda & -\Lambda & -\Sigma & & & & & -\Lambda & -\Lambda & -\Sigma & & & & & & & & & (p_{0^S} \chi_{1,-1}) \\ & & & & & & & & & & -\Lambda + \Sigma & & & & & & & & (p_{1^S} \chi_{1,1}) \\ & & & & & & & & & & & -\Lambda - \Sigma & & & & & & & (p_{-1^S} \chi_{1,-1}) \end{array} \quad (\text{A13})$$

In this matrix, we subtracted from all diagonal elements a constant-energy term  $E_g - E_{\text{ex}}$ , where  $E_g$  is the band-gap energy and  $E_{\text{ex}}$  is the exciton binding energy. Also, we used the abbreviated notations,  $\Lambda = \frac{1}{3}\lambda$ ,  $\Sigma = \frac{1}{2}(J_{k=0}^v + J_{k=0}^c) \langle S_z \rangle$ , and

$\Sigma' = \frac{1}{2}(J_{k=0}^v - J_{k=0}^c) \langle S_z \rangle$ . Thus, in the present formalism, the exciton energies are given in terms of four parameters  $\lambda$ ,  $\Delta$ , and  $J^v$ ,  $J^c$ . The experimental procedure to determine these adjustable parameters is described in the text.

<sup>1</sup>See, for example, G. Güntherodt, Phys. Cond. Matter **18**, 37 (1974), and the literature cited therein.

<sup>2</sup>T. Mitani and T. Koda, Phys. Lett. A **43**, 137 (1973).

<sup>3</sup>T. Mitani and T. Koda, in Proceedings of the Twelfth International Conference on the Physics of Semiconductors (Stuttgart, 1974), (unpublished), p. 889.

<sup>4</sup>See, for example, Y. Toyozawa, in Proceedings of the Tenth International Conference on the Physics of Semiconductors, Cambridge, 1970 (unpublished), p. 5.

<sup>5</sup>R. J. Zollweg, Phys. Rev. **111**, 113 (1958); G. A. Saum and E. B. Hensley, Phys. Rev. **113**, 1019 (1959).

<sup>6</sup>J. A. Krumhansl, in *Proceedings of the Photoconductivity Conference* (Wiley, New York, 1956), p. 455.

<sup>7</sup>E. Matatagui, A. G. Thompson, and M. Cardona, Phys. Rev. **176**, 950 (1968).

<sup>8</sup>Y. Toyozawa, Prog. Theor. Phys. (Kyoto) **20**, 53 (1958).

<sup>9</sup>Y. Onodera and Y. Toyozawa, J. Phys. Soc. Jpn. **22**, 833 (1967).

<sup>10</sup>H. B. Callen and E. Callen, Phys. Rev. **136**, A1675 (1964).

<sup>11</sup>F. Rys, J. S. Helman, and W. Baltensperger, Phys. Cond. Matter **6**, 105 (1967).

<sup>12</sup>R. J. Kearney, M. Cottini, E. Grilli, and G. Baldini, Phys. Status Solidi B **64**, 49 (1974).

<sup>13</sup>C. Haas, Phys. Rev. **168**, 531 (1968).

<sup>14</sup>G. Güntherodt, J. Schoenes, and P. Wachter, J. Appl. Phys. **41**, 1083 (1970).

<sup>15</sup>W. J. Scouler, J. Feinleib, J. O. Dimmock, and C. R. Pidgeon, Solid State Commun. **7**, 1685 (1969).

<sup>16</sup>A. Yanase and T. Kasuya, J. Phys. Soc. Jpn. **25**, 1025 (1968), Prog. Theor. Phys. Suppl. **46**, 388 (1970); T. Mitani, M. Ishibashi and T. Koda, J. Phys. Soc. Jpn. **38**, 731 (1975).